

Knots as Topological Order Parameter for Semi-Flexible Polymers

Martin Marenz* and Wolfhard Janke†

Institut für Theoretische Physik, Universität Leipzig, Postfach 100 920, D-04009 Leipzig, Germany

Using a combination of the replica-exchange Monte Carlo algorithm and the multicanonical method, we investigate the influence of bending stiffness on the conformational phases of a bead-stick homopolymer model and present the pseudo-phase diagram for the complete range of semi-flexible polymers, from flexible to stiff. Although a simple model, we observe a rich variety of conformational phases, reminiscent of conformations observed for synthetic polymers or biopolymers. Changing the internal bending stiffness, the model exhibits different pseudo phases like bent, hairpin or toroidal. In particular, we find thermodynamically stable knots and transitions into these knotted phases with a clear phase coexistence, but almost no change in the mean total energy.

PACS numbers: 87.15.-v, 02.70.Uu, 05.70.Fh, 02.10.Kn

Since the first simulation of knotted polymers in 1975 [1], the occurrence and behavior of knots in polymers has been studied in various contexts. Scanning through protein data bases has revealed that several proteins form knots [2–4]. In particular, Virnau et al. [5] have reviewed the whole Protein Data Bank (<http://www.pdb.org> [6]) and identified 36 different proteins forming relatively simple knots, none of which features more than five crossings – somehow evolution tries to avoid knotted proteins [7]. On the other hand, flexible polymers form much more complicated knots, which occur by chance in the swollen [8–10] and in the collapsed phase [10, 11]. Essential for the existence of these two phases is the excluded volume and attraction of the monomers. Already lattice polymer simulations [12, 13] show that models integrating self-avoidance and attraction exhibit a swollen, a globular, and a frozen phase. In this work we go a step ahead and investigate the knottedness of semi-flexible bead-stick polymers. There exists already some works concerning the more complex phase space of polymer models that incorporate bending stiffness [14]. The most comprehensive study uses a model for semi-flexible polymers of bead-spring type with finitely extensible nonlinear elastic (FENE) bonds [15]. By varying the bending stiffness, these models are able to mimic a large class of polymers, exhibiting, for instance, bent, hairpin or toroidal conformations.

Nevertheless, none of the former work considered the knottedness of the polymer over the full bending stiffness range, which we will discuss in this Letter. By measuring the knot type we found pseudo phases with thermodynamically stable knotted polymers. The knot type will be shown to be an ideal topological order parameter to identify the knotting transition and, moreover, the behavior at the transition from an unknotted to a knotted pseudo phase turns out to be surprisingly different from all other pseudo-phase transitions of the bead-stick polymer in that it does not fit into the common classification scheme of first- and second-order phase transitions.

To model a coarse-grained polymer with an adjustable stiffness, we use a modified version of the bead-stick model of Refs. [16–18], which neglects the hydrophobicity of

the monomers. The model then consists of N identical monomers connected by bonds with length one. Non-adjacent monomers interact via the Lennard-Jones potential

$$E_{\text{LJ}} = 4\epsilon \sum_{i=1}^{N-2} \sum_{j=i+2}^N \left[\left(\frac{\sigma}{r_{ij}} \right)^{12} - \left(\frac{\sigma}{r_{ij}} \right)^6 \right], \quad (1)$$

where r_{ij} is the distance between two monomers. The parameters ϵ and σ are set to one for the rest of this work, i.e., energies are measured in units of ϵ and lengths in units of σ . The stiffness is modeled through the cosine potential adopted from the well-known discretized worm-like chain model [19] and defined by

$$E_{\text{bend}} = \sum_{i=1}^{N-2} (1 - \cos \theta_i), \quad (2)$$

where θ_i represents the angle between adjacent bonds. The complete Hamiltonian is then given by $E = E_{\text{LJ}} + \kappa E_{\text{bend}}$, where κ parametrizes the strength of the bending term compared to the Lennard-Jones potential.

Topological barriers between the knotted phases forced us to apply relatively complex Monte Carlo algorithms in order to obtain reliable results. To simulate the system in the complete (T, κ) -plane, we used two complementary Monte Carlo algorithms. The first is a combination of the parallel multicanonical method [20, 21] and a one-dimensional replica exchange [22] in the κ direction (PMUCA+RE). The second is a two-dimensional version of the replica-exchange method (2D-RE), which simulates the system in T and κ direction in parallel. By means of a two-dimensional weighted histogram analysis algorithm [23], we are able to calculate the canonical mean values for every point in the (T, κ) -plane within the simulated parameter ranges. To generate well equilibrated results it was necessary to apply quite intricate bridge-end and double-bridging moves that respect the fixed bond-length constraint, besides the common crankshaft, spherical-rotation and pivot moves. The results of both methods, PMUCA+RE and 2D-RE, are in good agreement with each other.

To determine the structural phases we measured the total energy $\langle E \rangle$, both sub-energies $\langle E_{LJ} \rangle$ and $\langle E_{\text{bend}} \rangle$, the squared end-to-end distance $\langle R_{ee}^2 \rangle$, the squared radius of gyration $\langle R_g^2 \rangle$, and the eigenvalues of the gyration tensor $\langle \lambda_1 \rangle, \langle \lambda_2 \rangle, \langle \lambda_3 \rangle$. The derivatives with respect to temperature of these observables mark the locations of the different pseudo-phase transitions, which should not be mistaken with phase transitions in the thermodynamic limit ($N \rightarrow \infty$). The different observables give slightly different results for finite systems, so that the transitions are smeared out. Additionally, we performed microcanonical analyses as a complementary approach to identify the different pseudo-phase transitions. These are based on the microcanonical entropy, $S(E) = k_B \ln \Omega(E)$, with $\Omega(E)$ being the density of states. In the microcanonical framework a peak in the derivative of the microcanonical inverse temperature $d\beta_{\text{micro}}(E)/dE$, which is itself the derivative of the entropy, $\beta_{\text{micro}}(E) = dS(E)/dE$, corresponds to a pseudo-phase transition. A detailed description of the framework can be found in Ref. [24]. Although it is expected that all but the collapse and freezing transitions vanish in the thermodynamic limit, they still determine the structural behavior of short and midrange polymers and are important for understanding the behavior of mesoscopic systems.

The stiffness-dependent behavior of the bead-stick model [Eqs. (1), (2)] for chains with $N = 14$ and 28 monomers is summed up in the pseudo-phase diagrams shown in Fig. 1, which are constructed from the surface plots of all measured thermal derivatives and the results of the microcanonical analysis. The black lines in Fig. 1 mark the thermally most active regions and represent the location of the pseudo-phase transitions. For high temperatures, where the system is entropy dominated and the polymer resembles a discretized worm-like chain, the conformations are either gaseous-like and extended (E) or rod-like (R). When the temperature is lowered, the Lennard-Jones energy becomes more important and the polymer collapses. One can clearly distinguish two different regimes. For small κ the polymer behaves similarly to a flexible chain with collapsed (C) and frozen (F) pseudo phases. This contrasts with larger κ , where the polymer undergoes a first-order-like transition from the unstructured state (R) to states with differently structured motifs (DN, H, KC_n). For clarity, we omitted in Fig. 1 some sub-phases, where the shape parameters and the microcanonical analysis suggest additional pseudo-phase transitions between differently shaped conformations of the same motif. Especially, the frozen phase F subsumes many different crystal-like phases which differ only in minor aspects.

To identify the knotted phases, we measured the knot type of the polymer, which turns out to be an ideal order parameter. In principle, the knot type, denoted by C_n , defines which smooth closed curves can be transformed into each other by applying multiple Reidemeister moves.

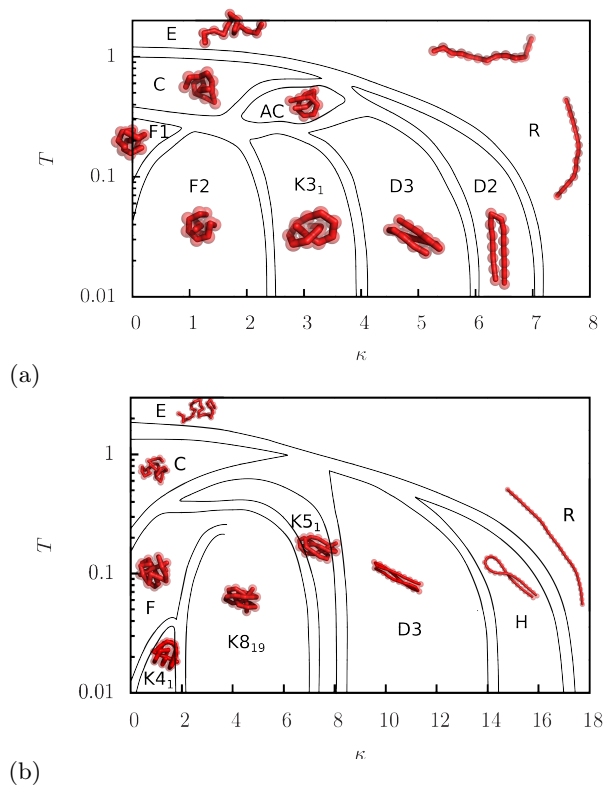


FIG. 1. (color online) The black lines sum up all signals of the thermal derivative of all measured observables for (a) 14 monomers and (b) 28 monomers. The pseudo phases are labeled as follows: E - elongated, R - rod-like, C - collapsed (AC is an artifact of the small chain length, both termini of the polymer are aligned), F - frozen, KC_n - knotted phase with the corresponding knot type, DN - $(N - 1)$ times bent polymers, H - hairpin. We omitted some sub-phases of DN, $K8_{19}$, and F, which do not change the overall picture.

Practically, this means two knots are not of the same type if one of them cannot be deformed into the other without cutting and rejoining the curve. The integer number C counts the minimal number of crossings for any projection on a plane and the subscript n distinguishes topologically different knots with the same number of crossings. A detailed exposition of mathematical knot theory can be found in Ref. [25]. Of course, an open polymer cannot satisfy the mathematical definition of a knot, unless the termini are closed virtually. In this work we applied a closure which is inspired by tying a real knot. Both termini are connected by a straight line, which is enlarged in both directions to a point far outside the polymer. These new termini are then connected through a point which lies on a line perpendicular to the connecting line of the termini and which is also located far away from the center of mass of the polymer. We have tested our results with different other closures and obtained almost identical results. To calculate C_n , we employed a technique described in Ref. [26], which is based on a

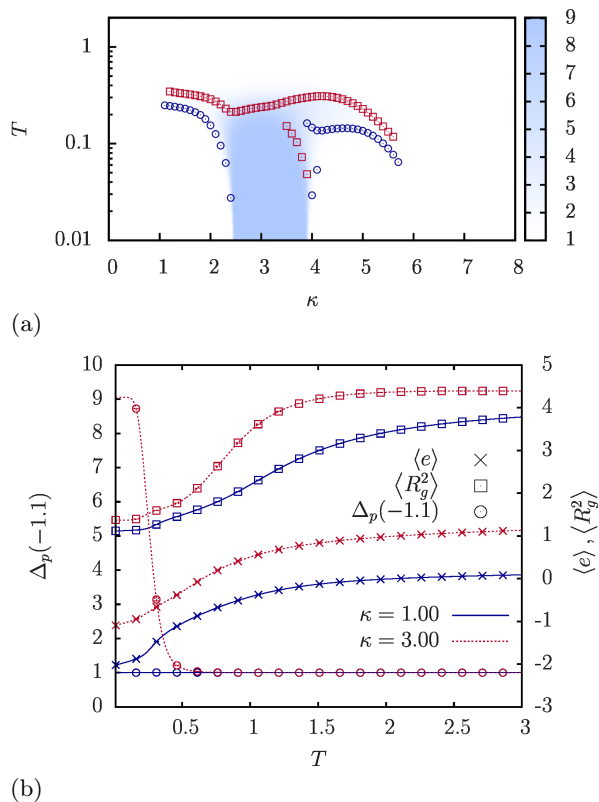


FIG. 2. (color online) (a) Surface plot of $\Delta_p(-1.1)$ over the complete (T, κ) -plane for a 14mer, blue circles correspond to maxima and red squares to minima of $\frac{d}{dT}\Delta_p(-1.1)$. The blue regime, $\Delta_p(-1.1) = 9.0546$, marks the $K3_1$ knot phase of the polymer. (b) Temperature profile of $\langle E/N \rangle$, $\langle R_g^2 \rangle$, and $\Delta_p(-1.1)$ at $\kappa = 1.00$ (blue solid lines) and $\kappa = 3.00$ (red dashed lines). In contrast to $\langle E/N \rangle$ and $\langle R_g^2 \rangle$, $\Delta_p(-1.1)$ differs significantly between the knotted ($\kappa = 3.00$) and unknotted ($\kappa = 1.00$) phase.

variant of the Alexander polynomial $\Delta(t)$,

$$\Delta_p(t) = |\Delta(t) \times \Delta(1/t)|, \quad (3)$$

evaluated at $t = -1.1$. $\Delta_p(t)$ inherits the ability to distinguish different knot types from the Alexander polynomial. Strictly speaking, the Alexander polynomial and likewise $\Delta_p(t)$ are not unique invariants. However, for simpler knots both generate unique results, and they are able to distinguish all knots found in this work.

In the knotted pseudo phases, marked with K in Fig. 1, the probability to find the corresponding knot is almost one. This means every measured polymer is of that knot type and implies that the knots are thermodynamically stable. We want to emphasize that this is different from the formerly investigated knots which form by chance in the swollen or collapsed phase. This makes $\Delta_p(-1.1)$ a perfect topological order parameter to distinguish knotted and unknotted phases, as is demonstrated in Fig. 2(a). In Fig. 2(b) one can see that the behavior of the mean total energy $\langle E \rangle$ and the squared radius of gyration $\langle R_g^2 \rangle$

is qualitatively very different at the knotting transition $AC \leftrightarrow K3_1$ ($\kappa = 3.00$) and the freezing transition $C \leftrightarrow F2$ ($\kappa = 1.00$). On the other hand, the knot parameter $\Delta_p(-1.1)$ clearly signals the pseudo-phase transition and goes from 1 (unknotted polymer) to 9.0546 (3_1 knot) only in the case of a transition into a stable knot. As expected, the 28mer (and even more the 42mer [27]) exhibits a richer phase diagram with more complicated knot types, see Fig. 1(b). However, the qualitative behavior at the phase boundaries turned out to be very similar so that we will focus in the following on the 14mer.

The knotting transitions from one structured state to another (e.g., $K3_1 \leftrightarrow D3$) are quite interesting. At first glance, one could assume that they behave first-order-like, similar to other solid-solid-like transitions at low temperatures. However, the microcanonical analysis indicates a second-order-like behavior by a peak in $d\beta_{\text{micro}}(E)/dE$ which is smaller than zero (not shown here). Likewise, the canonical probability distribution $p(E)$ does not exhibit a double-peak structure, see Fig. 3(a). On the other hand, the two-dimensional energy distribution $p(E_{\text{LJ}}, E_{\text{bend}})$ points to a phase coexistence. In Fig. 3(b) one can clearly identify two separate peaks, one corresponding to the knotted phase and the other to the unknotted phase. Surprisingly, both phases have almost identical mean total energy $\langle E \rangle$ at the coexistence point, and there is almost no signal in the total energy and heat capacity at the transition, see Fig. 4. We thus observe no latent heat where the polymer undergoes the transition into the knotted phase. Rather, the Lennard-Jones energy E_{LJ} and the bending energy E_{bend} are transformed into each other [28].

This behavior changes if the polymer enters the knotted phase from an unstructured conformation. For example, staying on the transition line between $K3_1 \leftrightarrow D3$ for $N = 14$ and going to higher temperatures, the two peaks in $p(E_{\text{LJ}}, E_{\text{bend}})$ start to merge until they form a single peak at the transition between $AC \leftrightarrow K3_1$, where the phase coexistence vanishes. This behavior is similar for all other observed knotting transitions.

The reason for the missing knotted phases in Ref. [15] is not rooted in this intricate behavior with “concealed” signals, however, but may rather lie in the choice of the bond length r_b and the minimum of the Lennard-Jones potential r_{min} which are identical in [15] but different by a factor of 1.22 in this work. We have tested a few parametrizations of bead-spring models and always observed thermodynamically stable knots except for the special parametrizations used in [15]. The observation that the polymer minimizes its total energy in bent conformations by maximizing the number of monomers located in the Lennard-Jones minima of other monomers suggests the following conjecture: if $r_b \approx r_{\text{min}}$ and the bonds are flexible enough, bent conformations are energetically so strongly favored that knotted states become unlikely.

In conclusion, we have investigated the complete stiffness dependent behavior of a semi-flexible bead-stick ho-

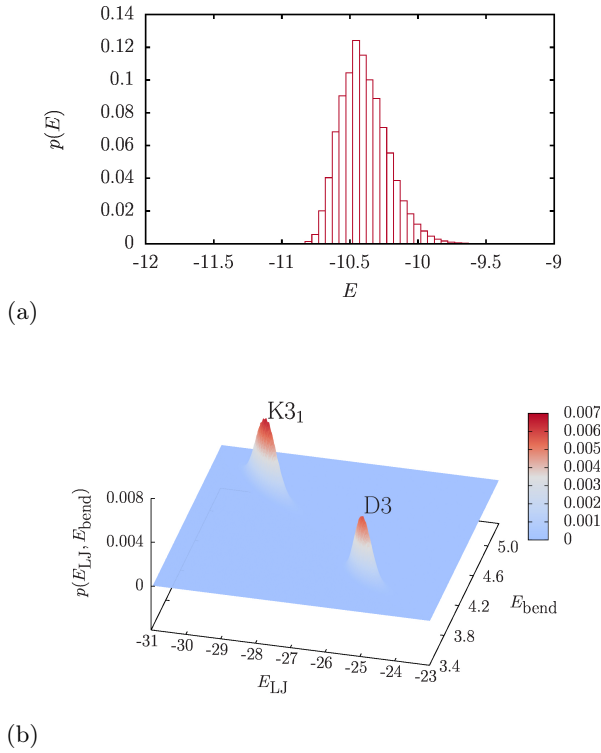


FIG. 3. (color online) Energy probability distribution of a 14mer at a point where $\frac{d}{dT} \Delta_p(-1.1)$ suggests a knotting transition ($\kappa = 3.9$ and $T = 0.0483$). Plot (a) shows the one-dimensional probability distribution $p(E)$. In (b) the energy is split into the two sub-energies, which leads to a double peak in the two-dimensional probability distribution $p(E_{LJ}, E_{bend})$. The left peak corresponds to the knotted state $K3_1$ and the right one to the bent state $D3$. The one-dimensional probability distribution is exactly the projection of $p(E_{LJ}, E_{bend})$ along the line connecting the two peaks, thus the phase coexistence is perfectly hidden in $p(E)$.

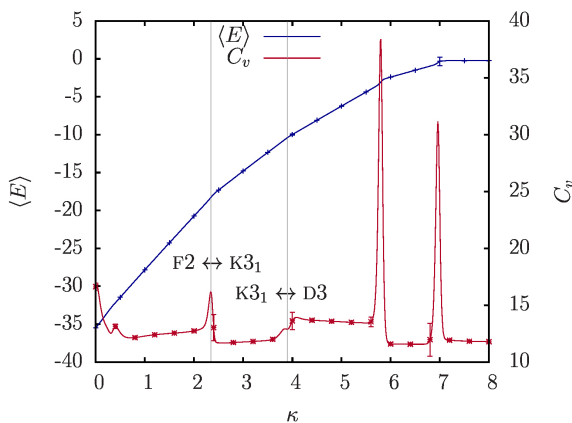


FIG. 4. (color online) Energy $\langle E \rangle$ and heat capacity C_v of a 14mer at $T = 0.0483$ over the complete range of investigated κ values. At both knotting transitions, $\kappa = 2.7 : F2 \leftrightarrow K3_1$ and $\kappa = 3.9 : K3_1 \leftrightarrow D3$, there is nearly no shift in the energy and therefore no signal in the heat capacity that is larger than the statistical error.

mopolymer. Besides the conformations already observed in previous works, we found pseudo-phase transitions into novel phases which are characterized by thermodynamically stable knots and showed that $\Delta_p(-1.1)$ is a perfect topological order parameter for these transitions. Moreover, at these topological transitions we found phase coexistence between structured phases but, surprisingly, with equal total mean energy in the two phases. The missing signal in the heat capacity implies a pseudo-phase transition with a clear phase coexistence but without latent heat. At the moment, investigating short single polymer chains in experiments seems unrealistic, and it appears even more unrealistic to observe structural properties such as knots. However, preparation and detection methods for single polymers at surfaces have recently made quite an impressive progress [29, 30], so that one can now resolve polymers of down to 20 monomers. A sensible next step could be hence an investigation of the influence of an adsorbing surface on the occurrence of stable knotted pseudo phases for a generic semi-flexible polymer. Later on, this could be extended to more realistic synthetic polymer models to guide experiments.

We would like to thank Johannes Zierenberg, Niklas Fricke, Stefan Schnabel, Jan Meischner, and Martin Treffkorn for many fruitful discussions. Computing time provided by the John von Neumann Institute for Computing (NIC) under grant No. HLZ21 on the supercomputer JU-ROPA at Jülich Supercomputing Centre (JSC) is gratefully acknowledged. This project has been funded by the European Union and the Free State of Saxony through the “Sächsische AufbauBank” and by the DFG (German Science Foundation) through SFB/TRR 102 (project B04) and the Graduate School GSC 185 “BuildMoNa”.

* martin.marenz@itp.uni-leipzig.de

† wolfgang.janke@itp.uni-leipzig.de

- [1] M. Frank-Kamenetskii, A. Lukashin, and A. Vologodskii, *Nature* **258**, 398 (1975).
- [2] M. Mansfield, *Nat. Struct. Mol. Biol.* **1**, 213 (1994).
- [3] W. R. Taylor, *Nature* **406**, 916 (2000).
- [4] R. C. Lua and A. Y. Grosberg, *PLoS Comput. Biol.* **2**, 0350 (2006).
- [5] P. Virnau, L. Mirny, and M. Kardar, *PLoS Comput. Biol.* **2**, 1075 (2006).
- [6] H. M. Berman, J. Westbrook, Z. Feng, Z. Gilliland, T. N. Bhat, H. Weissig, I. N. Shindyalov, and P. E. Bourne, *Nucleic Acids Res.* **28**, 235 (2000).
- [7] T. Wüst, D. Reith, and P. Virnau, *Phys. Rev. Lett.* **114**, 028102 (2015).
- [8] K. Koniaris and M. Muthukumar, *Phys. Rev. Lett.* **66**, 2211 (1991).
- [9] T. Deguchi and K. Tsurusaki, *Phys. Rev. E* **55**, 6245 (1997).
- [10] P. Virnau, Y. Kantor, and M. Kardar, *J. Am. Chem. Soc.* **127**, 15102 (2005).
- [11] R. Lua, A. L. Borovinskiy, and A. Y. Grosberg, *Polymer*

- 45**, 717 (2004).
- [12] U. Bastolla and P. Grassberger, *J. Stat. Phys.* **89**, 1061 (1997).
 - [13] J. Krawczyk, A. L. Owczarek, and T. Prellberg, *Physica A* **389**, 1619 (2010).
 - [14] H. Noguchi and K. Yoshikawa, *Chem. Phys. Lett.* **278**, 184 (1997).
 - [15] D. T. Seaton, S. Schnabel, D. P. Landau, and M. Bachmann, *Phys. Rev. Lett.* **110**, 028103 (2013).
 - [16] F. H. Stillinger, T. Head-Gordon, and C. L. Hirshfeld, *Phys. Rev. E* **48**, 1469 (1993).
 - [17] A. Irbäck, C. Peterson, F. Potthast, and O. Sommelius, *J. Chem. Phys.* **107**, 273 (1997).
 - [18] M. Bachmann, H. Arkin, and W. Janke, *Phys. Rev. E* **71**, 031906 (2005).
 - [19] M. Rubinstein and R. H. Colby, *Polymer Physics* (Oxford University Press, Oxford, 2003) p. 456.
 - [20] J. Zierenberg, M. Marenz, and W. Janke, *Comput. Phys. Commun.* **184**, 1155 (2013).
 - [21] B. A. Berg and T. Neuhaus, *Phys. Lett. B* **267**, 249 (1991); *Phys. Rev. Lett.* **68**, 9 (1992).
 - [22] K. Hukushima and K. Nemoto, *J. Phys. Soc. Japan* **65**, 1604 (1996).
 - [23] A. M. Ferrenberg and R. H. Swendsen, *Phys. Rev. Lett.* **61**, 2635 (1988); **63**, 1195 (1989).
 - [24] C. Junghans, M. Bachmann, and W. Janke, *Phys. Rev. Lett.* **97**, 218103 (2006).
 - [25] L. H. Kauffmann, *Knots and Physics*, 2nd ed. (World Scientific, Singapore, 1991).
 - [26] P. Virnau, *Physics Procedia* **6**, 117 (2010).
 - [27] Not shown here, because the details of the more complicated pseudo-phase diagram do not contribute to the understanding of the basic mechanism.
 - [28] This topological change also explains why we need PMUCA+RE or 2D-RE to overcome the topological barrier.
 - [29] S. Förster and W. Widdra, *J. Chem. Phys.* **141**, 054713 (2014).
 - [30] S. Förster, E. Kohl, M. Ivanov, J. Gross, W. Widdra, and W. Janke, *J. Chem. Phys.* **141**, 164701 (2014).